ESAG-2002

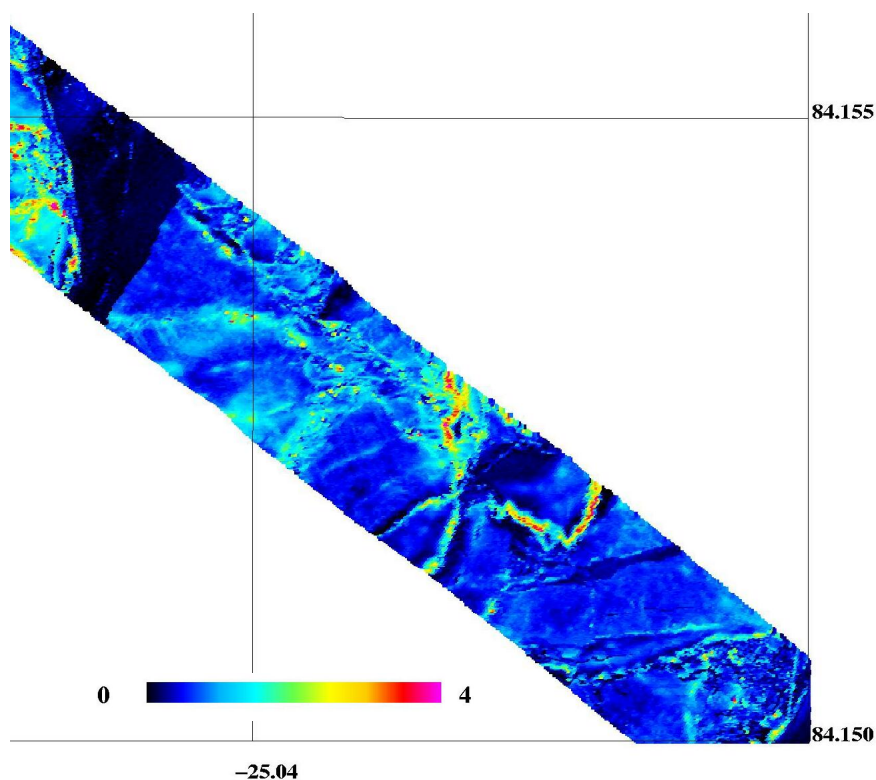## European airborne gravity and lidar survey in the Arctic Ocean

Final report
Dec 2002

by

R. Forsberg, K. Keller, S. M. Hvidegaard and A. Olesen
National Survey and Cadastre (KMS)
Denmark

Kort & Matrikelstyrelsen
National Survey and Cadastre - Denmark

esa

1. INTRODUCTION

The ESAG-2002 airborne gravity and lidar (laser scanner) campaign of the European Space Agency (ESA) and Kort og Matrikelstyrelsen (National Survey and Cadastre of Denmark, KMS) has been carried out in the period April 29 – May 19, 2002), with support from ESA and the Danish Natural Science Research Council.

The purpose of ESAG-2002 was:

- To acquire high-accuracy airborne gravity measurements of the Arctic Ocean, in support of ESA's GOCE mission, filling in voids in the existing gravity coverage in the polar region and providing control ties to older gravity surveys in the region.
- To acquire scanning laser ranging (lidar) data and profiling laser altimetry over the sea-ice north of Greenland, as a mean of measuring ice elevations, to provide background data in preparation for the ESA CryoSat mission.

The airborne survey was done using a chartered Air Greenland Twin-Otter aircraft (OY-POF), operating primarily from military airfields at Station Nord (Greenland) and Alert (Canada), as well as from Svalbard.

In addition to mapping of sea-ice by lidar, laser surveys were also done in profiles across the southern Greenland ice sheet (Kangerlussuaq to Kulusuk) as well as along selected parts of the East Greenland ice cap margin. These en-route surveys are not considered part of ESAG-2002, and have not yet been processed. Following the ESAG-2002 the aircraft and KMS crew continued to Hall Beach, Canada, for a cooperative NRCan-NIMA-KMS airborne gravity survey of the Foxe Basin, till May 2002 the last major gravity void in the Canadian Arctic.

Table 1. Summary of ESAG-2002 operations.

| April 26-29	Installation of scientific equipment in Air Greenland hangar at Kangerlussuaq. Test flight.
April 30-May 3	Lidar survey of East Greenland ice sheet margin, Kulusuk region. Ice sheet landings in different elevations for snow pit measurements. Flight from Kangerlussuaq to Station Nord, via Constaple Pynt airport. Laser survey of Geikie ice cap (repeat of earlier surveys 1996-1998). Laser survey of Greenland ice sheet margin and new islands off 79-glacier enroute.
May 4-9	First ESAG-2002 gravity flights from Station Nord. Overflights of Swedish ice breaker "Oden" on May 6 and May 9 in Fram Strait. Test flight and check of gravimeter in Svalbard.
May 10-16	Operations from Canadian Forces Station Alert. All lines flown as planned, in spite of aircraft generator fault, which resulted in aircraft non-availability for 2 days.
May 17	Flight from Alert to Thule Airbase via Nares Strait. Planned gravity/lidar profile over Greenland ice sheet margins could not be done due to clouds. End of ESAG-2002, aircraft continues to Canada.
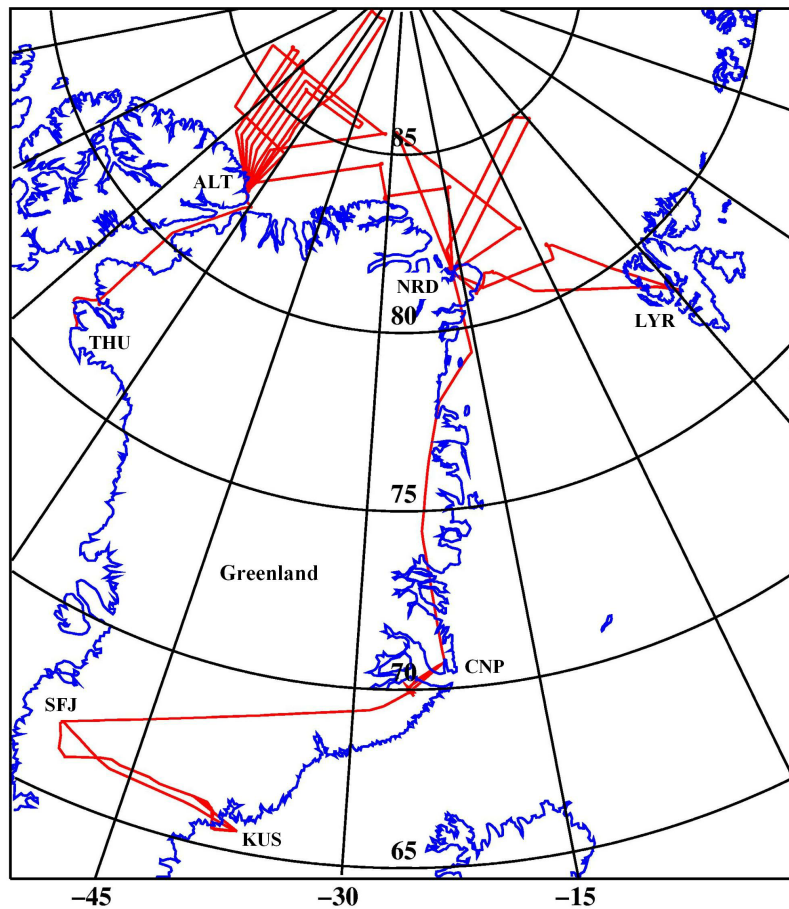
Fig .1. Flight tracks of ESAG-2002. SFJ = Kangerlussuaq base airport; operations bases
LYR = Longyearbyen, Svalbard; NRD = Station Nord, Greenland; ALT = Alert, Canada

The details of the field operations and science background may be found in the report "Progress report #2 – Field Operations", dated June 2002, and the detailed descriptions of the recorded raw data in the "Raw data acquisition report", dated September 2002. Track numbers are listed in Appendix 3.

This report mainly describes the processed GPS, gravity, and laser altimeter data for ice thickness measurement. These data have been enclosed on a CD-ROM as well.

The scanning lidar data processing is still underway, and is very much an area of active research. Due to the large volume of scanning lidar data (approx. 30 CD-ROMs of raw data), the final lidar-swaths of ice thickness are *not* included, but rather some examples of results are included, and a general recipe – and software – given on how to convert the scanning lidar data into ice free-board heights.

2. AIRCRAFT POSITION AND ATTITUDE PROCESSING

Aircraft GPS positions are fundamental for both airborne gravity and lidar processing.

The precise GPS positions of the two physical aircraft antennas were computed mainly using Trimble's software "GPSurvey" (v. 2.35) – keeping fixed the reference values of Table 2. Three separate geodetic dual-frequency GPS receivers (AIR1: Trimble 4000 SSI; AIR2: Ashtech Z-Surveyor; AIR3: Javad Legacy) were connected to the two antennas. All GPS data were recorded at 1 Hz.

Table 2 shows the used reference positions. The reference coordinates were computed using "AutoGipsy" of JPL and typically have an accuracy better than 5 cm in ITRF2000. (http://www.unavco.ucar.edu/data_support/processing/gipsy/auto_gipsy_info.html.)

Table 2. Reference GPS coordinates as computed by KMS.

Station	Lat	Lon	Ell. height	Comment
SFJ	67 00 21.6517	-50 42 9.6773	72.01	
KUS	65 34 40.5259	-37 9 11.9715	72.04	
NRD1	81 36 5.0977	-16 39 43.5273	70.04	
NRD2	81 35 49.7660	-16 39 24.8776	67.51	
LYR (8/5a)	78 14 51.4679	15 29 35.0743	52.52	*
LYR (8/5b)	78 14 51.4649	15 29 35.0779	52.56	*
LYR (9/5)	78 14 51.4646	15 29 35.0683	52.55	*
ALT1	82 30 41.5574	-62 19 36.3358	56.27	
ALT2	82 30 39.9955	-62 18 55.6712	42.81	
THU	76 32 16.4222	-68 47 48.0292	43.88	*
CNP	70 44 40.2403	-22 38 53.4847	70.77	*

* Only one file used to determine position

At least two independent aircraft GPS solutions were made by combinations of different reference stations and antenna. It is estimated that the GPS solutions are generally accurate at the 20-30 cm level r.m.s., for an example see fig. 3. The GPS conditions of 2002 were generally OK, with relatively few problems due to ionospheric problems. An example of the aircrafts natural phugeoid motion is shown in Fig. 2.
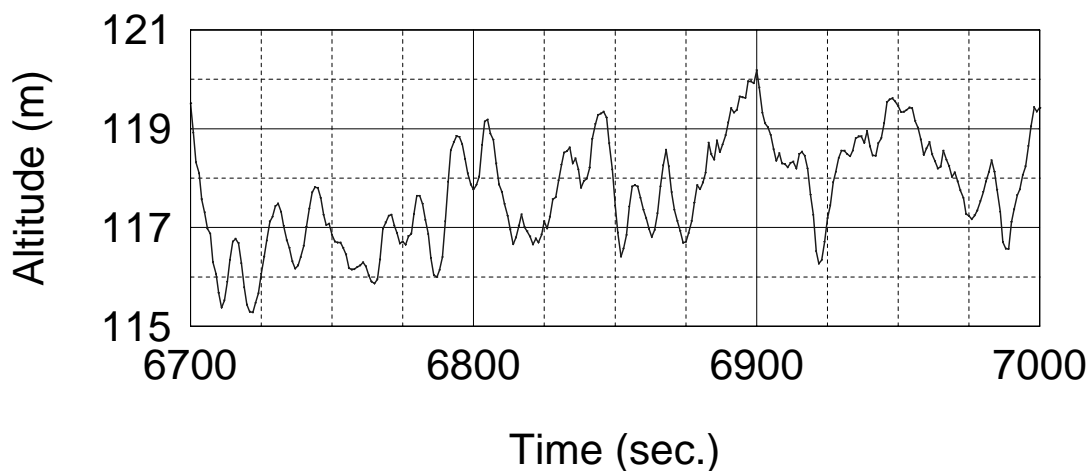

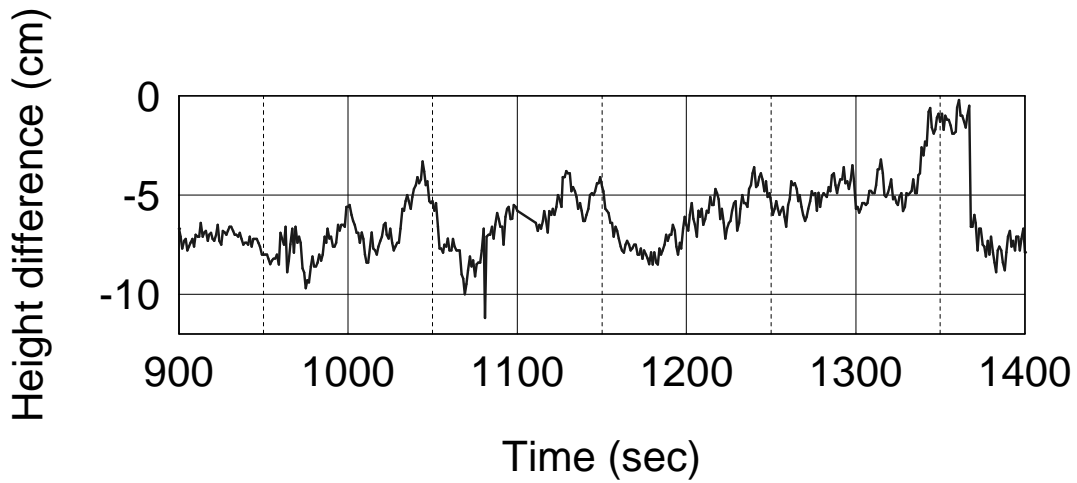*Fig. 2. Example of aircraft height during survey flight. Phugeoid motion of aircraft is seen.*

Fig. 3. Example of difference in height determination of AIR1 from different references (May 6).

GPS solutions were included in the raw data files provided to ESA September 2002.

Attitude data (roll, pitch and heading) are obtained from the Honeywell H-764G INS, an embedded GPS-INS military inertial navigation system. The INS was initialized for 5-8 minutes prior to the survey, allowing the system to align and find the north direction by gyro compassing. Gyrocompassing was successful in all cases, despite the northern latitudes (Alert, 82°N).

The H-764 generates output data both in free-inertial and Kalman-filtered GPS-INS mode. The pitch and roll differences between these two modes were generally below a fraction of a degree, and thus fully satisfactory for laser pointing and GPS antenna coordinate transfer to the lasers and the gravimeter sensor. Fig. 4 shows an example of roll and pitch variations during survey flight.
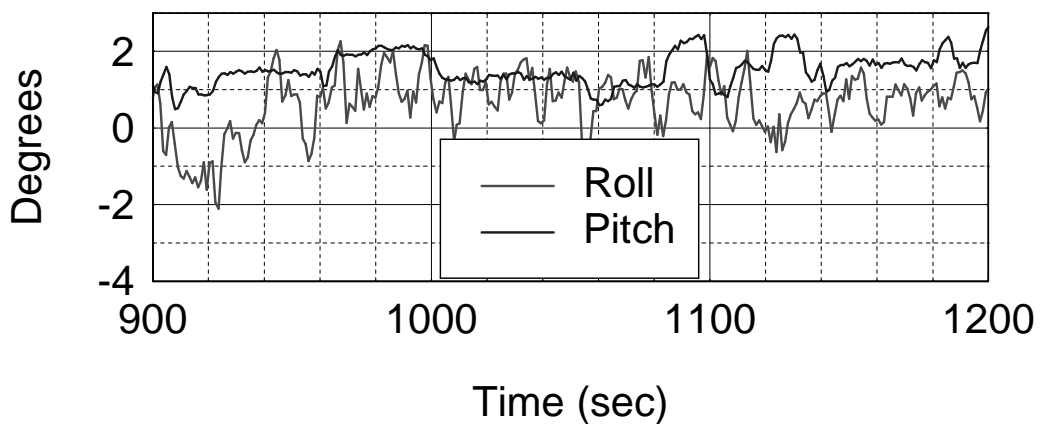

Fig. 4. Example of pitch and roll during straight-line survey (May 6)

The attitude data are time tagged in UT due to the embedded GPS receiver in the H-764 INS. The merging of GPS positions with raw H-764G ("EGI") INS data is done with a program "GPSEGI", that reads the raw Honeywell data files (.ddk files), logged at 50 Hz on a laptop PC through a 1553 military data bus interface.

The combined GPS-INS result files are in the form

Id, lat, lon, h, heading, pitch, roll

The Id is the time in UT in decimal hours. The heights h are by default ellipsoidal heights. To convert to height above the geoid the EGM-96 geoid model is routinely used. Alternative geoid models, based on the Arctic Gravity Project, may also be used. All geoid models are stored in GRAVSOFT grid formats (E-W rows from N to S, with a label header defining lat/lon limits and spacing).

An alternate inertial measurement unit – the Greenwood IMU – was also running and collecting data at 18 Hz during ESAG-2002. This unit is an experimental strapdown IMU sensor with fibre optics gyros. The unit served as a back-up unit, and have not been further utilized for ESAG-2002, since the H-764G functioned without problems.

3. AIRBORNE GRAVITY RESULTS

The airborne gravity data used raw gravity data from the S-99 gravimeter, as synchronized by the "READSYNC" programme to correct for the spring tension drifts of the 2002 survey due to some hardware problems, cf. 'raw data acquisition report'. The corrected raw data files are equivalent to conventional raw data files, and the loss of accuracy by the manual spring tension synchronization is estimated to be below 0.2 mgal r.m.s.

The Lacoste and Romberg "S" gravimeter uses a combination of two internal measurements - spring tension and beam velocity - to obtain the relative gravity variations. The gravity sensor is mounted on a gyro-stabilized platform, kept horizontal by a feed-back loop with two horizontal accelerometers and two gyros. Details of the operation principle of the LCR gravimeter can be found in Valiant (1991).

The basic gravimeter observation equation for relative gravity y is of the form

$$y = sT + kB´ + C \qquad\qquad (1)$$

where T is spring tension, s the scale factor, B´ the velocity of the heavily damped gravimeter beam, and the factor k the beam velocity/acceleration scale. A beam-type gravimeter like the S-meter is sensitive to horizontal accelerations even when the platform is levelled, and a cross-coupling correction C is computed in real time by the gravimeter control computer. For the S-99 the following factors were used: $s = 0.9967$ mGal/CU and $k = 29.3$ mGal/(mV/s). The latter value was determined by an autoregression technique between measurements and GPS accelerations. The value is in good agreement with laboratory measurements.

Free-air gravity anomalies at aircraft level are (omitting second order terms) obtained by

$$\Delta g = y - h'' - \delta g_{eotvos} - \delta g_{tilt} - y_0 + g_0 - \gamma_0 + 0.3086\,(h - N) \tag{2}$$

where h'' is the GPS acceleration, δg_{eotvos} the Eotvos correction (computed by the formulas of Harlan, 1968), y_0 the basereading, g_0 the apron gravity value, γ_0 normal gravity, h the GPS ellipsoidal height and N the geoid undulation (EGM96 used throughout). The platform off-level correction δg_{tilt} is expressed as

$$\delta g_{tilt} = y_{obs} - [y_{obs}^2 + A_x^2 + A_y^2 - a_x^2 - a_y^2]^{1/2} \tag{3}$$

where 'a' and 'A' denotes horizontal kinematic aircraft accelerations and horizontal specific forces measured by the platform accelerometers, respectively. Because of the potential high amplitude of horizontal accelerations, and the small difference between accelerations from accelerometer and GPS measurements, computed tilt effect is quite sensitive to the numerical treatment of the data. Calibration factors for the accelerometers have been determined by a FFT technique due to the frequency dependent behaviour of the platform, cf. Olesen et al. (1997).

Basereadings of the survey were very consistent, with negligible drift, allowing an independent check on the quality of basereadings before and after flights. The reference gravity values used in the airports were based on relative ties to the absolute gravity precision nets of Svalbard, Greenland and Canada, and are generally better than 0.1 mgal. The reference gravity values, forming the basis of the airborne gravity survey, are listed below.

ESAG-2002 gravity reference gravity values

Longyearbyen, Svalbard (apron)	982962.94 mgal
Station Nord (Garage)	983068.75 mgal
Alert apron (Hilton building)	983127.49 mgal

Lowpass filtering plays a fundamental role in airborne gravity processing. The objective of the filtering is both to account for the difference in filtering inherent from the data, and to remove the high frequency noise masking the gravity anomaly signal. The gravimeter data acquisition system uses a 1 sec. boxcar filter on internal 200 Hz data, whereas the inherent filtering of the accelerations derived from the GPS positions depends on the GPS processing software, and the algorithm applied for differentiation. This difference in filtering has little impact on the linear terms in our processing algorithm, because of the heavy final filtering. But the non-linear terms, mainly represented by the tilt correction, are quite sensitive to the initial filtering.

A typical processing output file is shown in Fig. 5. All data were filtered with a symmetric second order Butterworth filter with a half power point at 200 seconds, corresponding to a resolution of 6 km (half-wavelength). The impulse response and spectral behaviour of the used filter are shown in Fig. 6.
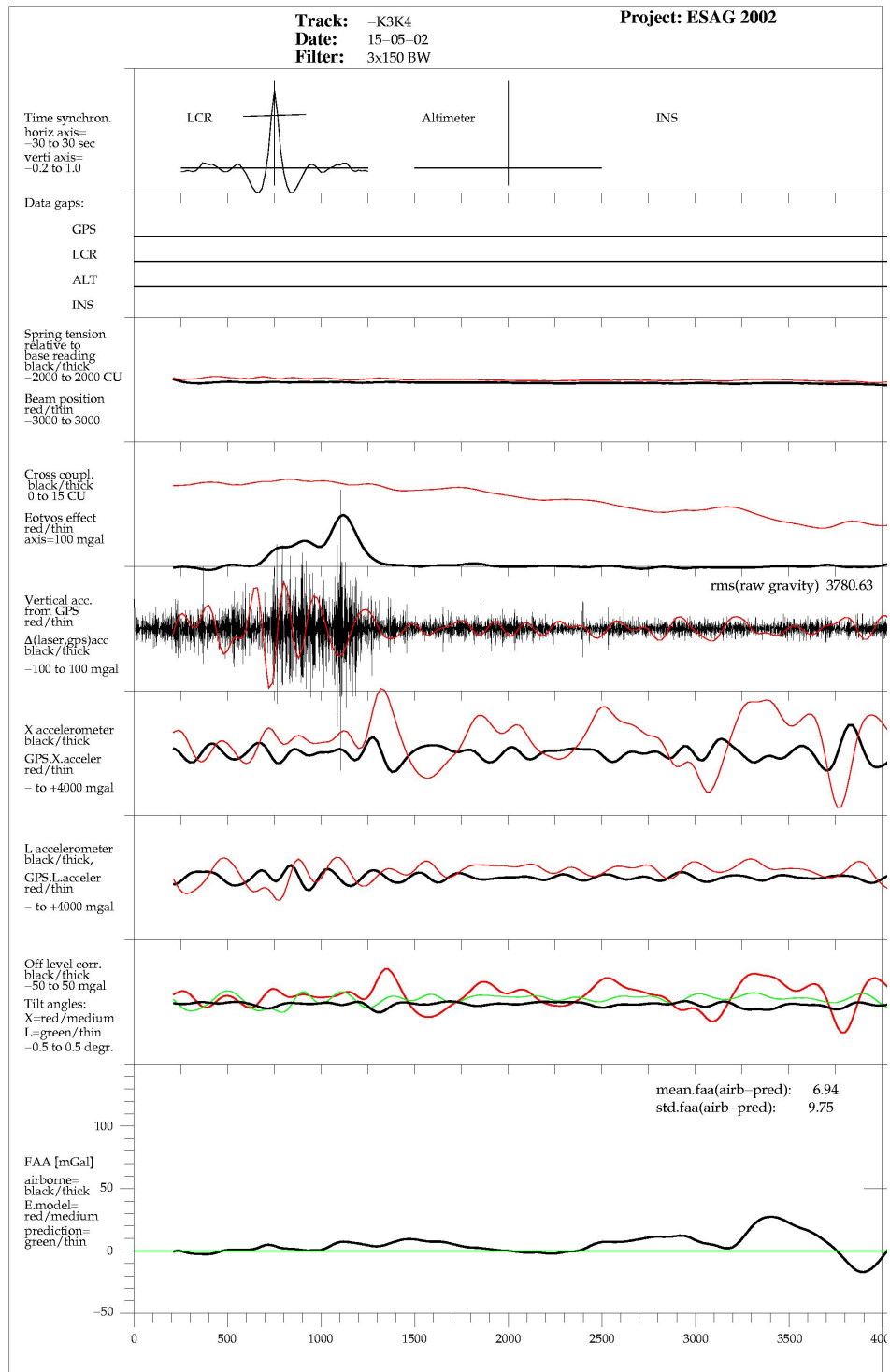
Fig. 5. Typical graphical example of line processing. The plots show from top to bottom the raw gravimeter data, accelerations from GPS, tilt corrections and the final gravity anomalies.
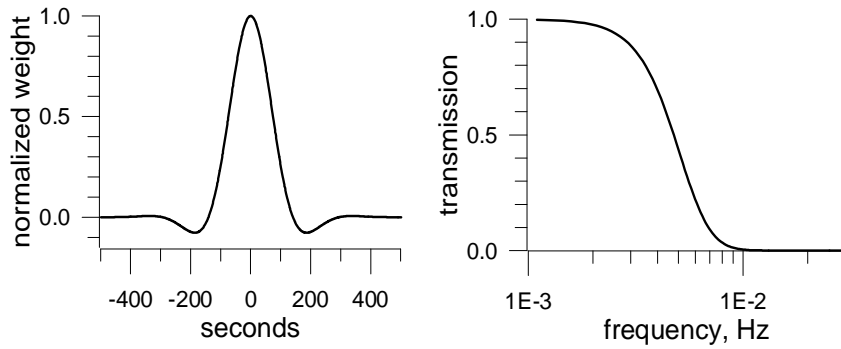
8

Fig. 6. Impulse response (normalized) and spectral representation of the filter

The results of the processing resulted in more than 95% of all flights being successful. Processing could be extended on the lines to within ca. 3 minutes of the line end. Data are presented in file format in the form

id, lat, lon, H, g, Δg, time (JD)

where *id = lineno*1000 + running no,* H the orthometric height, g absolute gravity and Δg the GRS-80 free-air gravity anomaly.
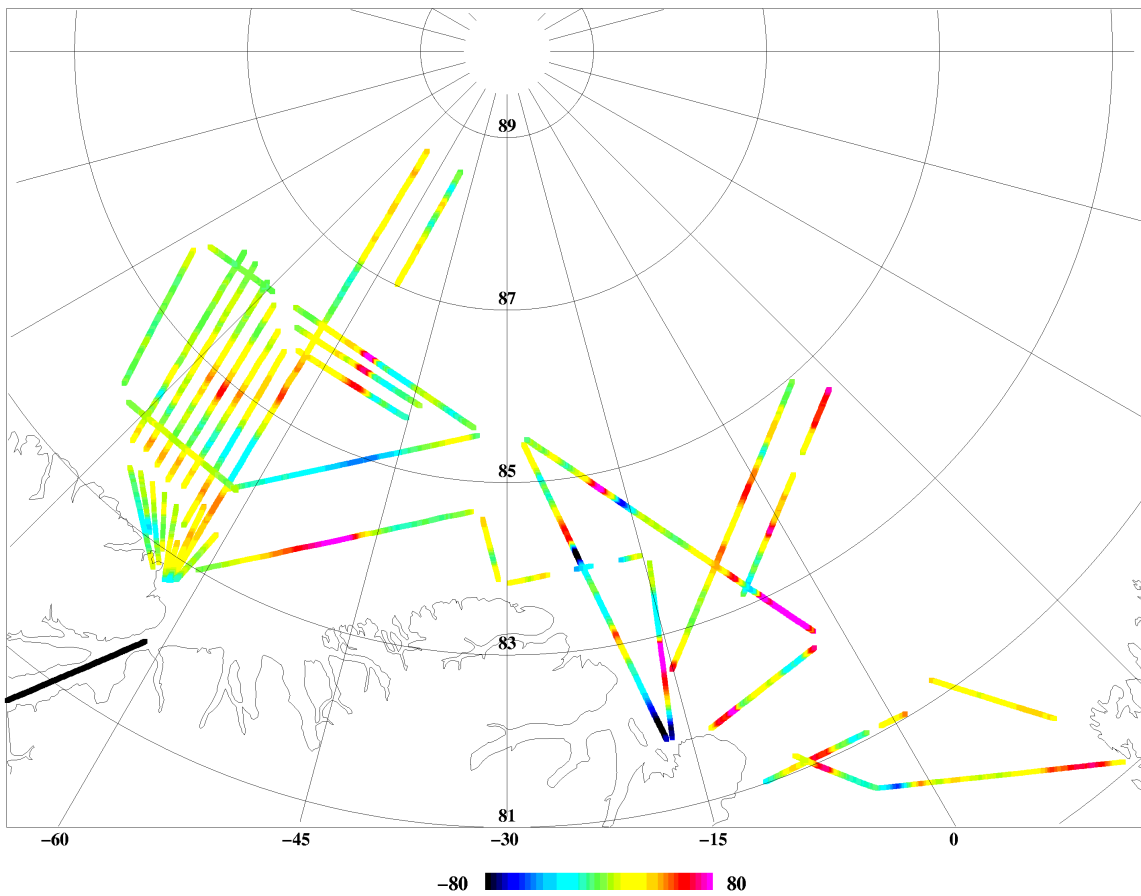

Fig. 7a. ESAG-2002 free-air gravity anomaies (mgal)

The final track data were evaluated by a bias-only cross-over adjustment. This showed a standard deviation of

$$\sigma = 2.4 \text{ mgal}$$

Assuming that the track noise is uncorrelated, the estimate of the noise on individual tracks would be $2.7/\sqrt{2} = 1.7$ mgal. We therefore estimate that the survey results are good to 2 mgal r.m.s. with a resolution of 6 km. It should be pointed out that *no* cross-over adjustment was applied to the final data. Fig 7a and 7b shows the final ESAG-2002 free-air anomaly data by itself and merged with other data.
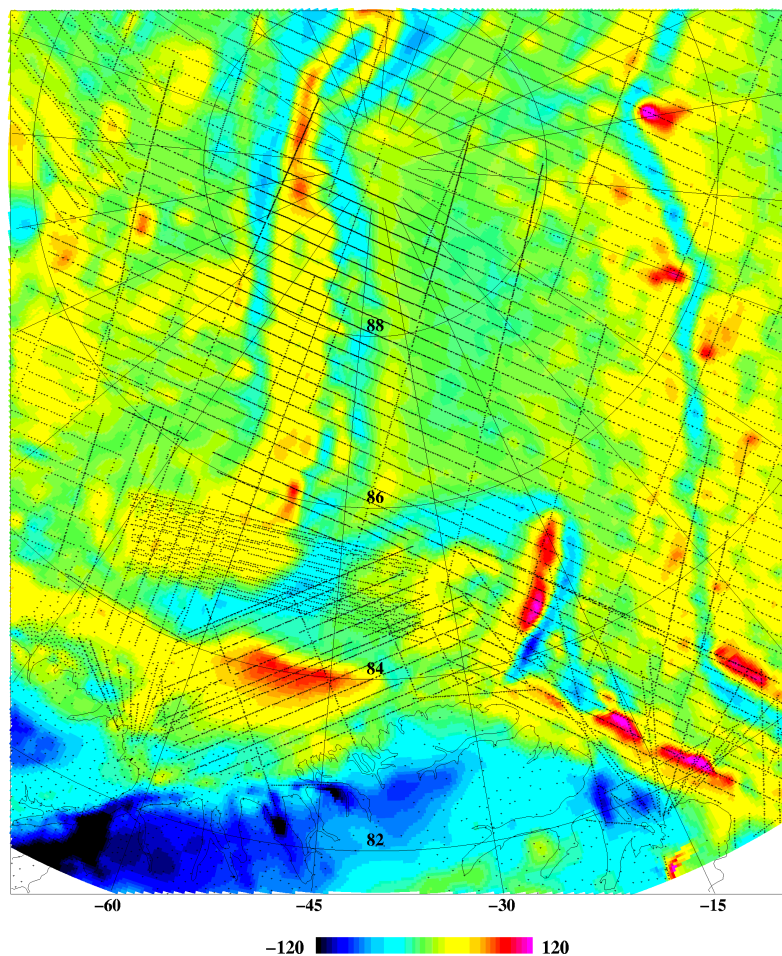

Fig 7b. Composite free-air anomalies (Bouguer on land) north of Greenland. Locations of airborne gravity data from KMS, NRL and PMAP shown. Major anomalies are associated with the main bathymetric features (Lomonossov Ridge and Morris Jesup Rise)

For an external data comparison, the ESAG-2002 data were compared to earlier collected airborne data:

1) The US Naval Research Laboratory 1998-99 data, collected north of the ESAG-2002 area by long survey lines from Svalbard (proprietary data, data provided by J. Brozena, NRL). The NRL data were collected at 2000 ft flight elevation, but due to larger aircraft speed filtered more heavily than the ESAG-2002 data.

2) Airborne gravimetry of the PMAP 1998 Canadian/German airborne geomagnetics survey (the smaller area NE off Alert with dense tracks). The PMAP aerogravity data have been provided by J. Halpenny, Geodetic Survey Division, Canada. The estimated standard deviation is 5 mgal.

3) KMS airborne gravity data 1998-2001 (1998 data only in Lincoln Sea). These data were processed using the same methods as ESAG-2002.
4) Airborne gravity data collected 1997-99 by the Alfred Wegener Institute, Germany, as part of the NORDGRAV and NOGRAM projects. The data was provided by T. Boebel, AWI, and are preliminary.

The comparisons were done by predicting from the KMS data sets at the location of the other data sets, comparing only values within short distance (less than 2 or 3 km). Table 3 shows the statistics of this comparison for the different other data sets, as well as the internal KMS data set consistency. Fig. 8 shows the location and magnitude of the misfits between the KMS 1998-2002 airborne surveys and the NRL 1998-99 surveys. It is not straightforward to do this comparison due to different flight elevations and filtering applied. In areas with a large gravity field variability (Lomonossov Ridge and Morris Jesup Rise) the large gradients of the gravity field will give relatively higher discrepancies between the surveys than in the gravitationally more smooth areas. Overall, however, the consistency of the data sets are good, and biases reasonably small.
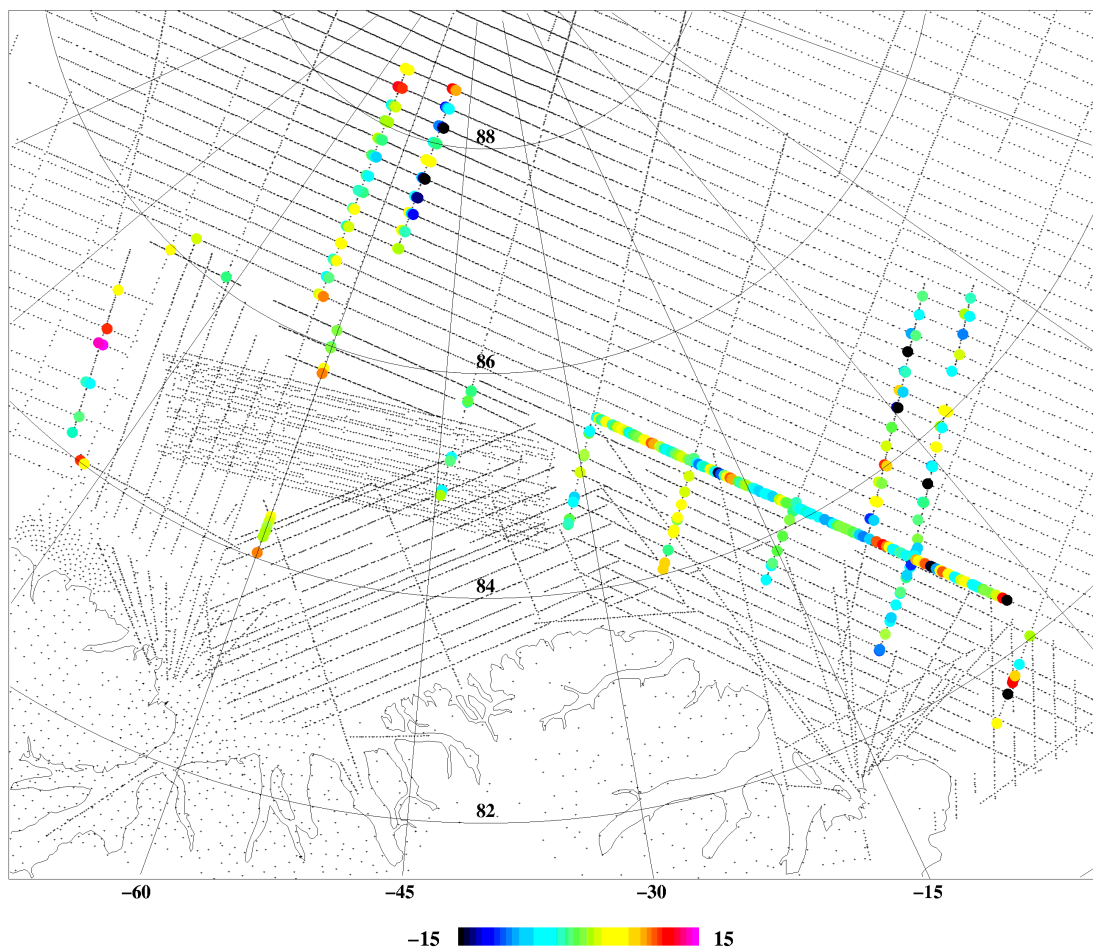

Fig. 8. Comparisons of ESAG-2002 data and NRL 1998-1999 airborne arctic data. Unit: mgal.

Table 3. Comparisons between different airborne gravity data sets in the Arctic Ocean (unit: mgal)

Data set	mean	std.dev.	min	max
ESAG-02 internal cross-overs	-0.1	2.4	-4	6
ESAG-02 vs. KMS1998-2001	-0.8	3.7	-16	13
ESAG-02 vs. NRL 1998-99	-0.5	5.8	-19	16
ESAG-02 vs. PMAP	1.2	5.1	-17	15
ESAG-02 vs. AWI	-5.8	11.2	-84	95

4. ICE FREE-BOARD HEIGHTS FROM LASER ALTIMETER DATA

Data from a single-beam Optech "Rangefinder" infrared laser unit was logged on the Greenwood data logger at 100 Hz. The unit only provided useful data for less than half of the tracks, due to log fog, cold, or open water. The 1000 ft flight elevation is close to the maximum range of the unit. The laser altimeter data was supplemented with the vertical component of the lidar data, in some cases where the Optech unit did not provide returns, and the Riegl scanner did. More details of the lidar data can be found in the next chapter.

To reduce noise and data volume all laser altimeter data is averaged to 10 Hz, which correspond to 7 m along track ground resolution. Each laser range measurment has a footprint of approx. 1 m.

The processing of the laser altimeter data involve the several steps:

1) Finding ellipsoidal heights of sea-ice surface using GPS position, attitude angles and laser range.
2) Obtain sea-surface heights above geoid using geoid model
3) Adjust for geoid, GPS, laser and sea-surface errors by adjusting smooth "lowest level" curve on results.

This can be combined into equation 4, that describes the recovery of the freeboard height, F:

$$F = h_{GPS} - H_{laser} - N - \Delta h \qquad (4)$$

Here h_{GPS} is the height of the aircraft above the WGS84 reference ellipsoid determined by GPS, H_{laser} the laser range corrected for roll and pitch from INS, and N the geoid height taken from a geoid model derived from previous KMS airborne gravity surveys. Δh are deviations of the sea surface from the geoid caused by errors on the geoid model and changes in the sea surface topography due to tides and permanent sea surface topography. Also included in Δh are errors from possible laser offsets and misalignments and GPS errors. Δh is removed by filtering. The filtering is done by fitting a second order polynomial to the minimum values of the dataset since these minimum values corresponds to open water or newly refrozen areas. Final freeboard heights are found by subtracting the filter from the heights above the geoid.

Fig. 9 shows an example of the recovery of the sea-ice freeboard heights for a 250 km long track. The top black curve is freeboard heights after filtering, the bottom grey curve is heights before filtering and the bottom black curve is the filter polynomial.
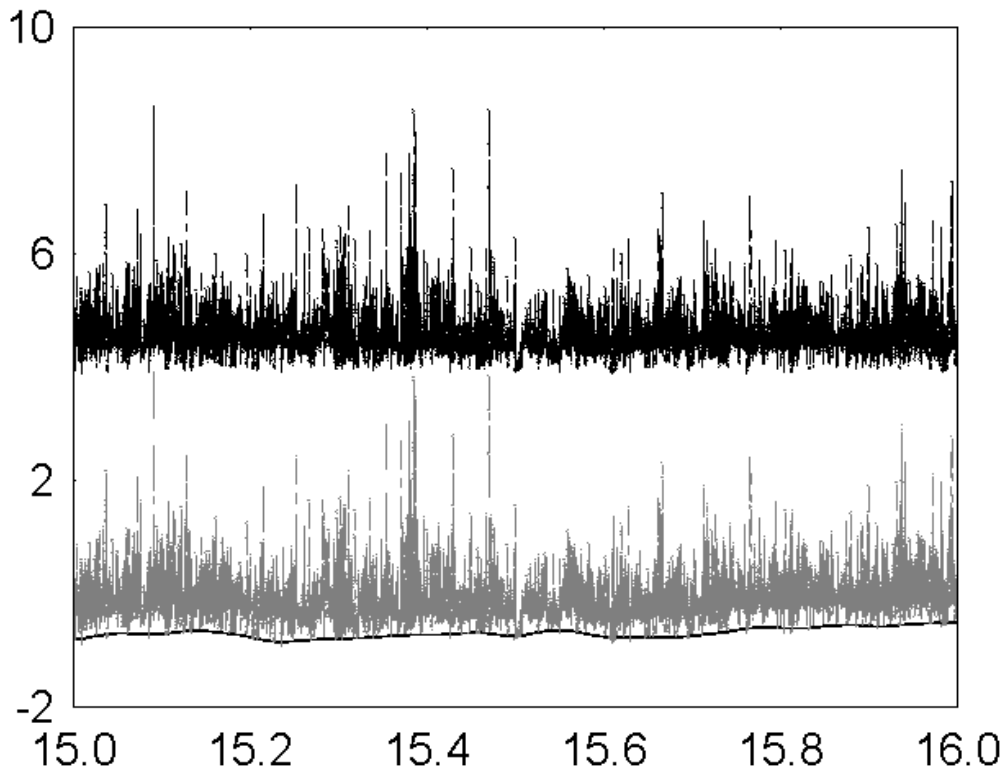
*Fig. 9. Sea-ice freeboard heights, top:before (shifted by 4 m on the y-axis);
bottom: after filtering; bottom black curve shows the lowest-value filter*

The sea-ice freeboard heights are converted into ice thickness using an assumption of equilibrium on scales longer than typical ice flow size (50-200 m). The principle is outlined in Fig. 10 and equation 5.

$$T = K * F \qquad with \qquad K = 1 + \frac{\rho_i h_i + \rho_s h_s}{h_i(\rho_w - \rho_i) + h_s(\rho_w - \rho_s)} \qquad (5),$$

with parameters as shown in Figure 10.

K=5.89 is used for this dataset based and is based on a model by Wadhams et al. (1992). This value for K is valid from April 30 to May 31. The presence of snow on the sea-ice is a major uncertainty for the k-factor, and the accuracy of the method cannot be fully utilized until improved models of snow depth could be obtained.

T is found for 4 km along track averages and shown in Figure 11 as a weighted mean gridded surface. This is only sensible since data from adjacent tracks are obtained within a few days. One should keep in mind the spatial variations of the drift velocities in the surveyed areas, which ranges from 15 cm/sec. in the Fram Strait decreasing to zero near Alert.
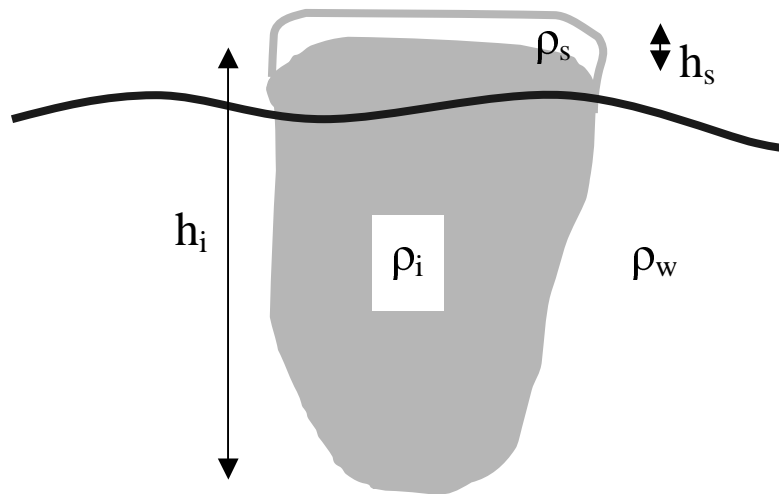
Fig. 10. Sea ice thickness determination principle

Fig. 11 displays the results of the sea-ice thickness determination from ESAG-2002 laser data. The missing tracks (compared to Fig. 1) are mainly due to fog and haze.
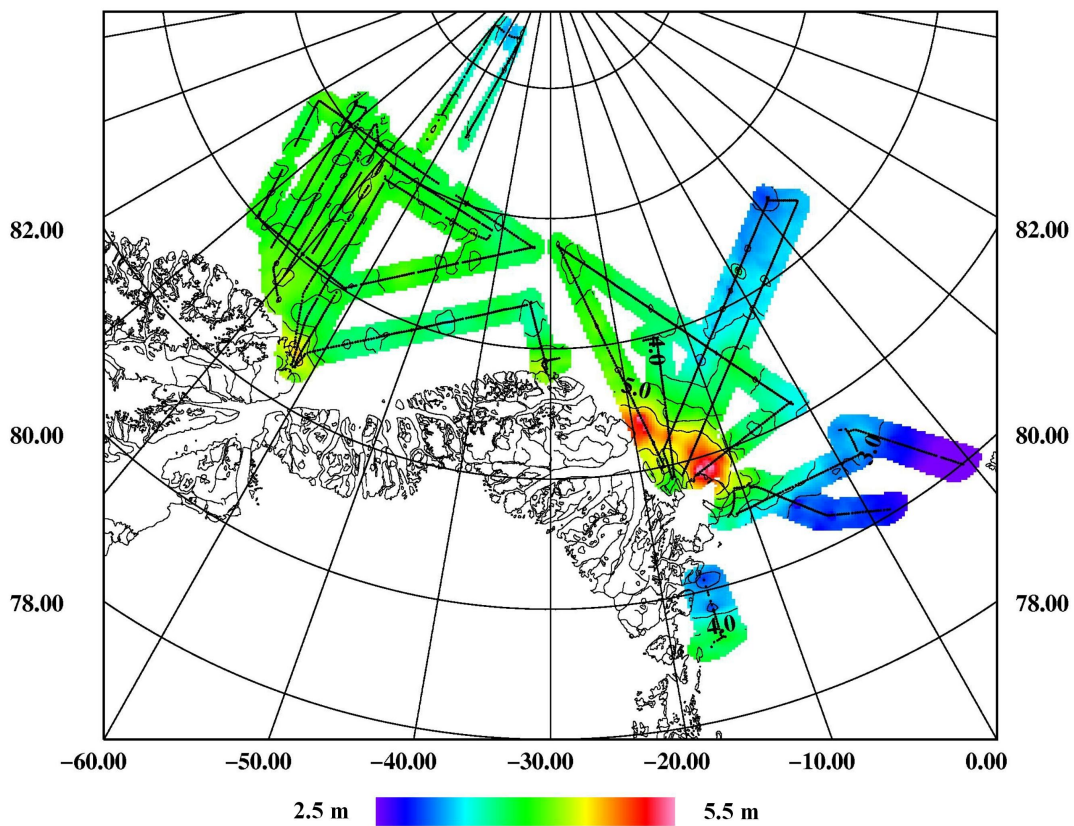

Fig. 11. Ice thickness for May 2002, based on ESAG-2002 data.

In June 1998, August 1999 and May 2001 ice thickness data were collected using the same methods as piggy-back operations for airborne gravity. Fig. 12 shows the results for the different years, with gridding by weighted mean interpolation. The maps are showing the thick ice in the Lincoln Sea, North-West of Greenland, and the relatively thinner ice in the Fram Strait region, East of Greenland. A direct trend from year to year is difficult to quantify due to the seasonal variations in ice thickness and the limited coverage of the airborne tracks.
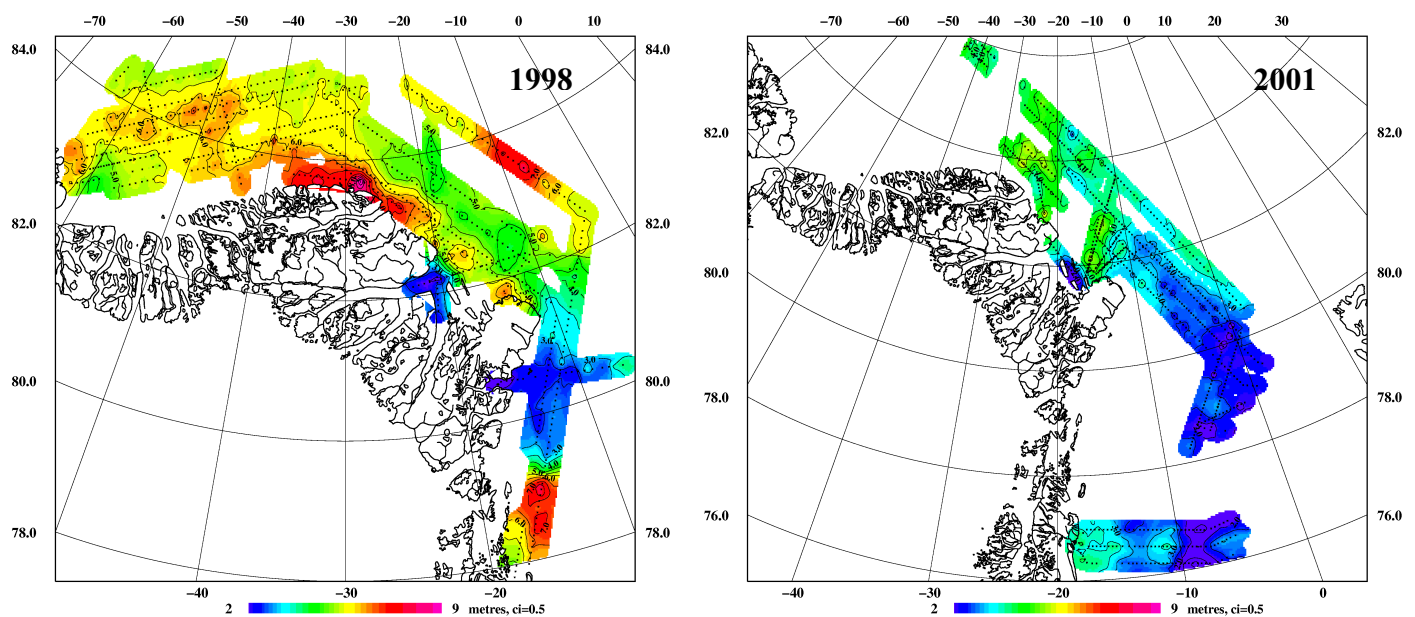

Fig. 12. Ice thickness maps from laser altimetry 1998 and 2001.

5. RIEGL SCANNING LIDAR SWATH ICE DATA

The swath lidar data provide approx. 200 samples of ice heights across the flight direction at a rate of 40 Hz. This results in ice free-board heights at a resolution of approx. 1.5 m in a 300 m wide swath (equal to the flight altitude) along the flight direction, by similar principles as the processing of laser altimeter data.

The KMS Riegl Q140 laser scanner (lidar) data was logged as hourly files on a stand-alone laptop computer. The lidar files are time tagged by a 1 pps signal from the AIR1 GPS receiver, with start time of the scans given by the operator as a file name. Due to some instrument problems the Riegl files has the risk of 1-sec time shifts, which may occur during the hourly files. It is therefore recommended to avoid such shifts by processing the Riegl data in small batches, no longer than a few minutes (this also limits the very voluminous data!).

Raw lidar files are stores with names referring to the time they were started. The details of the logged lidar data can be found in Appendix I.

The raw lidar files may be converted into elevations above the sea surface by the following programs:

1) READSCAN – reads the raw lidar file, and produce ice-surface heights, using an optional geoid model. Note: The raw lidar files are in three possible formats: two binary and a text format. Great care should be excised in reading the files. Generally files with ".2dd" termination are OK binary.

2) FITLIN – this program will fit a minimum surface to a laser swath data, providing (approximate) freeboard heights.

The program "PSE" may produce plots of the freeboard heights, either in lat/lon or as strips of data with along-track time as y-coordinate and a corresponding x-track time.

Sample input file for the READSCAN software (May 26 overflight of Repulse Bay, Canada):

```
201000.2dd
..\egi\gpsegi.pos   ! a GPS-INS position file with attitude info
..\..\egm96n.gri    ! a geoid model (GRAVSOFT grid)
scan.out
vert.out
20 10 00            ! scan start time
20.2 20.4           ! wanted time interval in dechr2
0 90 -90 90         ! geographic limits
5 5 t t t t f       ! nave ithin lbin lnew lpr lcalib lgeo
0 0 1.66            ! ant offset
-4 -1.3 0           ! pitch0 roll0 hdg0
```

The boresight/offset angles have been determined during the test flight over the buildings in Kangerlussuaq April 29th . Before flight, the corners at the roof of a box-shaped buliding were surveyed in order to calibrated the offset angles between the INS and the laser scanner. By flying in a four-leaf clover figure over the building the angles can be well determined. This is not yet automated and very much research in progress.

Sample input data for FITLIN (May 9):

```
scan.out            ! input file
scan.dat            ! output file for plotting
0.002 0.5 t         ! dtmin, rejl, lcut
```

The figures 13-15 below show a number of examples of scanner data as plotted with pse. Work is ongoing to derive statistical properties of the ice thickness data. The lidar scanner also has an amplitude channel. This may occasionally provide a clear resolution of structures in thin new ice.

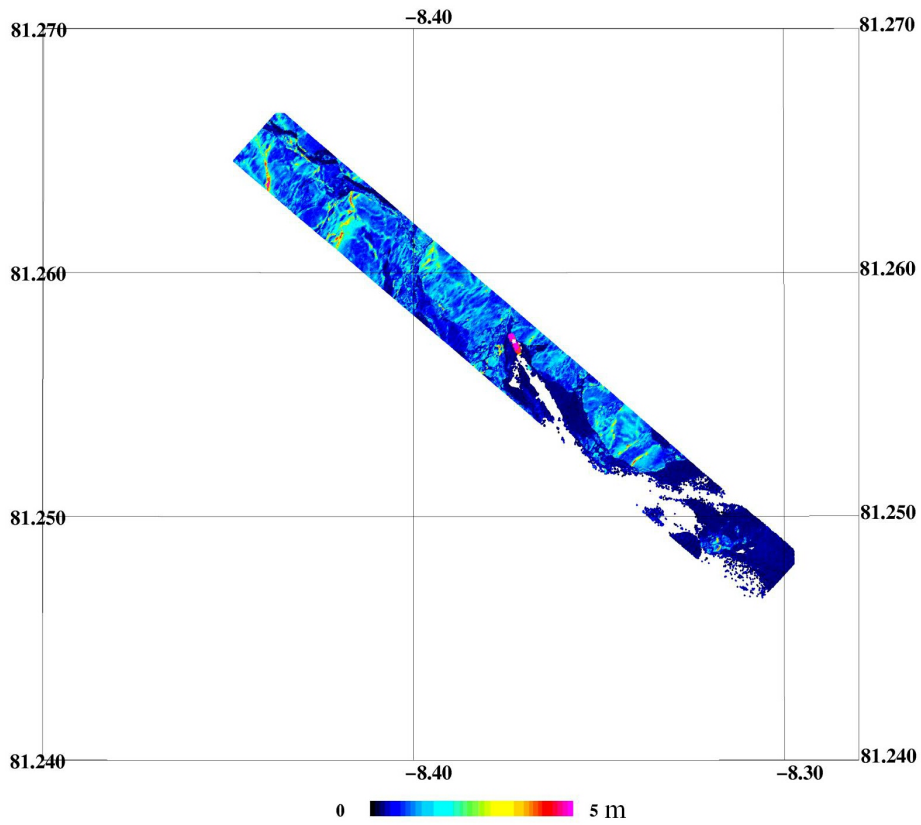*Fig. 13. May 9 – ODEN overflight(ice thickness).*
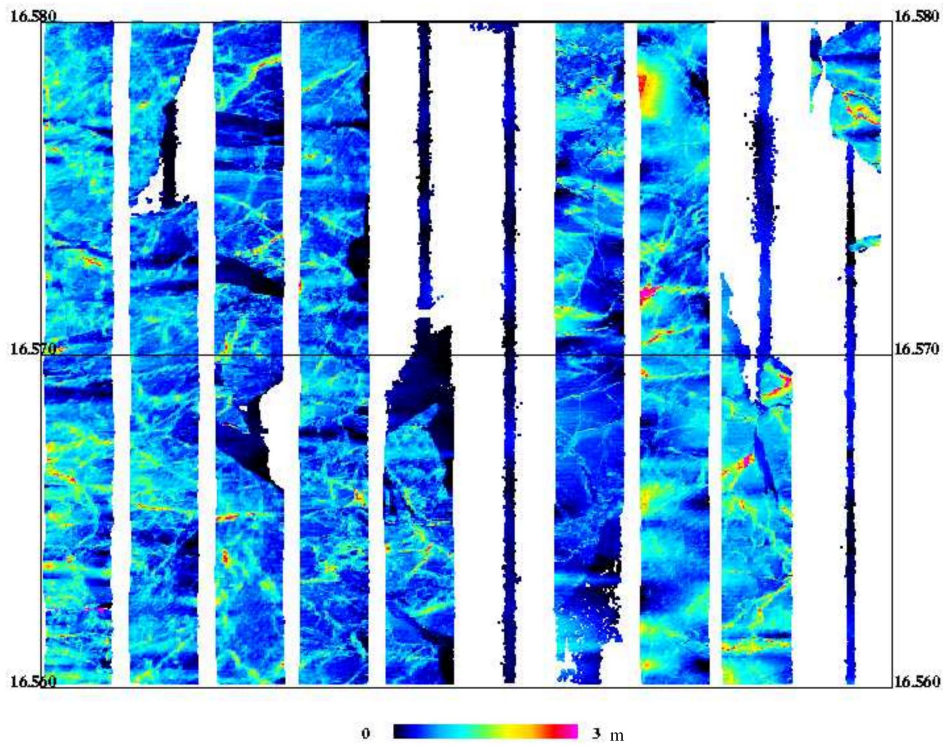
Fig. 14 Example of 12 minute lidar sequence freeboards (Fram Strait, May 9, startingat 16.56 dechr).Strips are continous from left to right. Open-water stretches are seen as narrow return band.
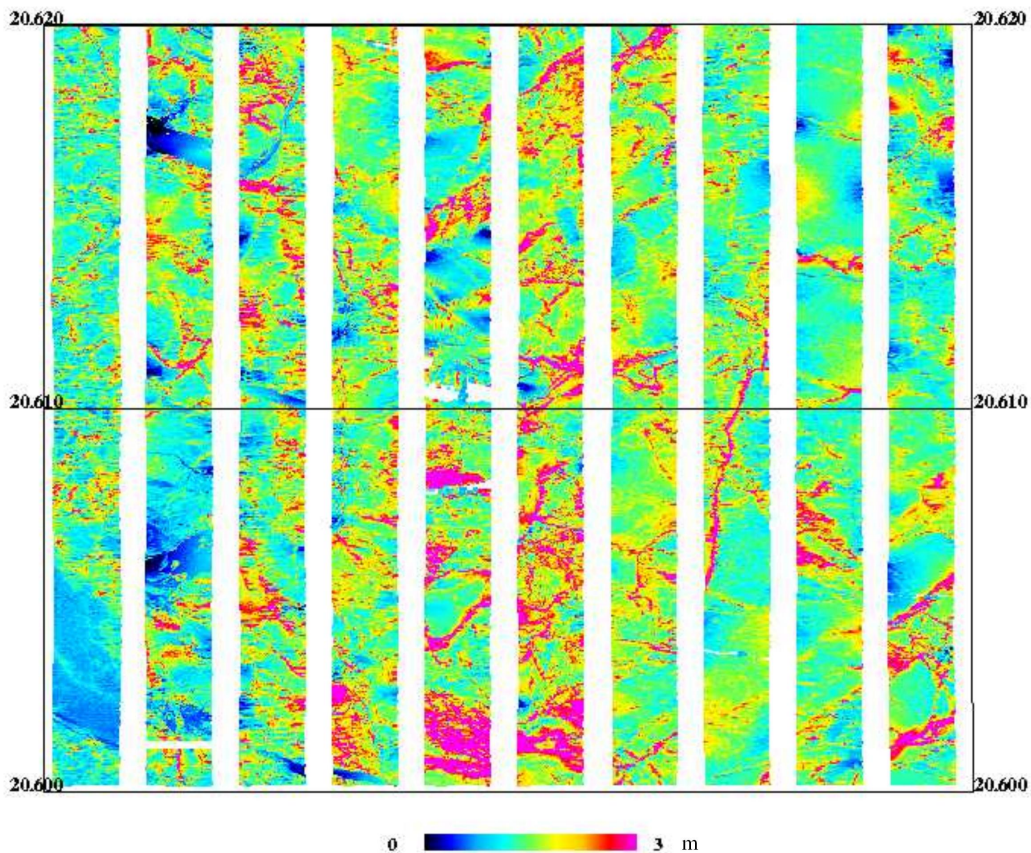
Fig. 15. Sea-ice freeboard heights in compact ice area north of Alert (May 15, 12 min from decimal hour 20.60)

6. AUXILLARY COMPARISON DATA: ICE DRILLING AND SHIPBORNE VIDEO

On-board video:
Approximately 30 1hr DV-tapes were recorded using a video camera looking out the right-hand side window of the aircraft. Five examples of video clips in mpeg-format are given on the final result CD.

Table 4. Approximate latitude/longitude of video sequences, Lincoln Sea

File name	Approximate lat/lon (DD MM.M)	
e1755.mpg	84 15.7 N	44 23.6 W
gf1520.mpg	86 05.3 N	52 21.3 W
gf1647.mpg	85 00.7 N	48 41.4 W
gf1736.mpg	83 59.8 N	62 20.8 W
i1828.mpg	86 58.2 N	55 15.2 W

The comparison of lidar scenes and video have not yet been performed.

Fig. 16. Left: Typical thick sea-ice. May 10 flight off north tip of Greenland (coastline in back-ground) Right: Typical thinner sea-ice further north in Polar Sea (May 12 north pole flight).

Ice thickness and density:

Limited reference measurements of sea-ice thickness, snow density and thickness were taken off Station Nord (on fast ice) and off Alert (on polar pack ice floes). The results are summarized in Table 6.
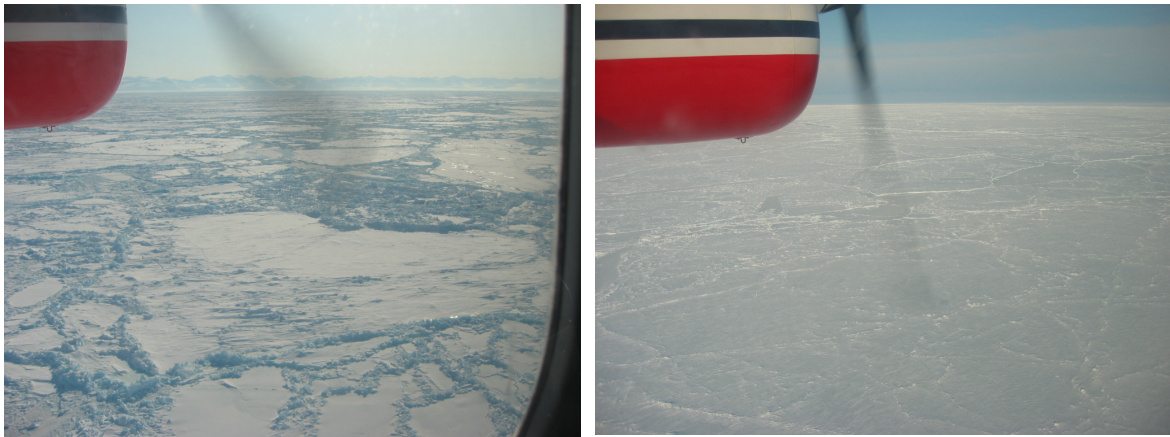
The measurements off Alert has a reasonably good agreement with the lidar scanner results, cf. Fig.18.

Table 6. Ice thickness measurements off Station Nord and Alert
(F is freeboard height, K freeboard to thickness conversion factor)

	Lat N	Lon W	Snow depth (m)	Snow +ice (m)	Snow density (g/cm**3)	F (m)	K
St. Nord	81 37.08	16 44.88	0.95	2.40	0.35	0.79	3.0
(fast ice)	81 38.22	16 49.86	0.68	2.21	0.30	0.64	3.5
Alert	82 32.01	62 09.64	0.50	4.50	0.32	0.77	5.8
(polar pack)	82 32.12	62 07.63	0.48	3.30	0.35	0.62	5.3
	82 32.25	62 05.28	0.35	3.00	0.35	0.51	5.9
	82 32.25	62.06.96	0.60	4.10	N/A	0.77	5.3
	82 32.26	62 07.25	0.70	5.10	0.35	0.93	5.5
	82 30.07	62 08.22	0.50	6.10+	N/A	(0.93)	(6.6)
Alert average			0.52	4.35+	0.34	0.71	5.6

Fig. 17. Ice drilling off Alert and Station Nord
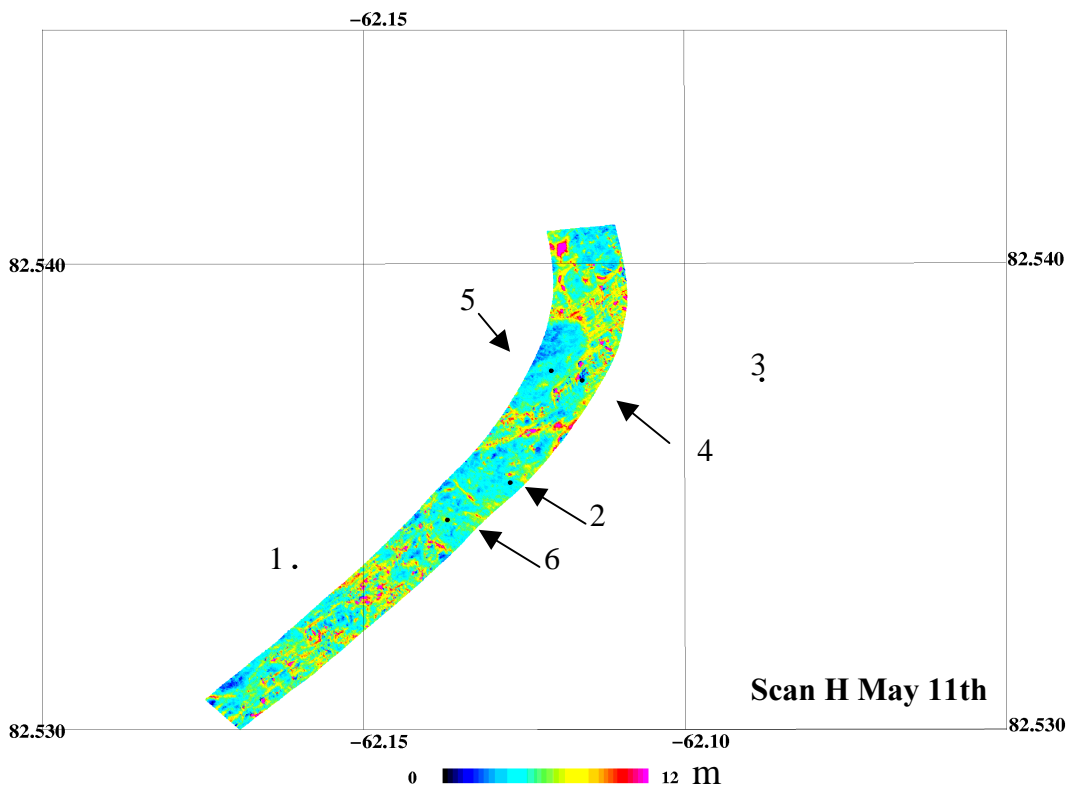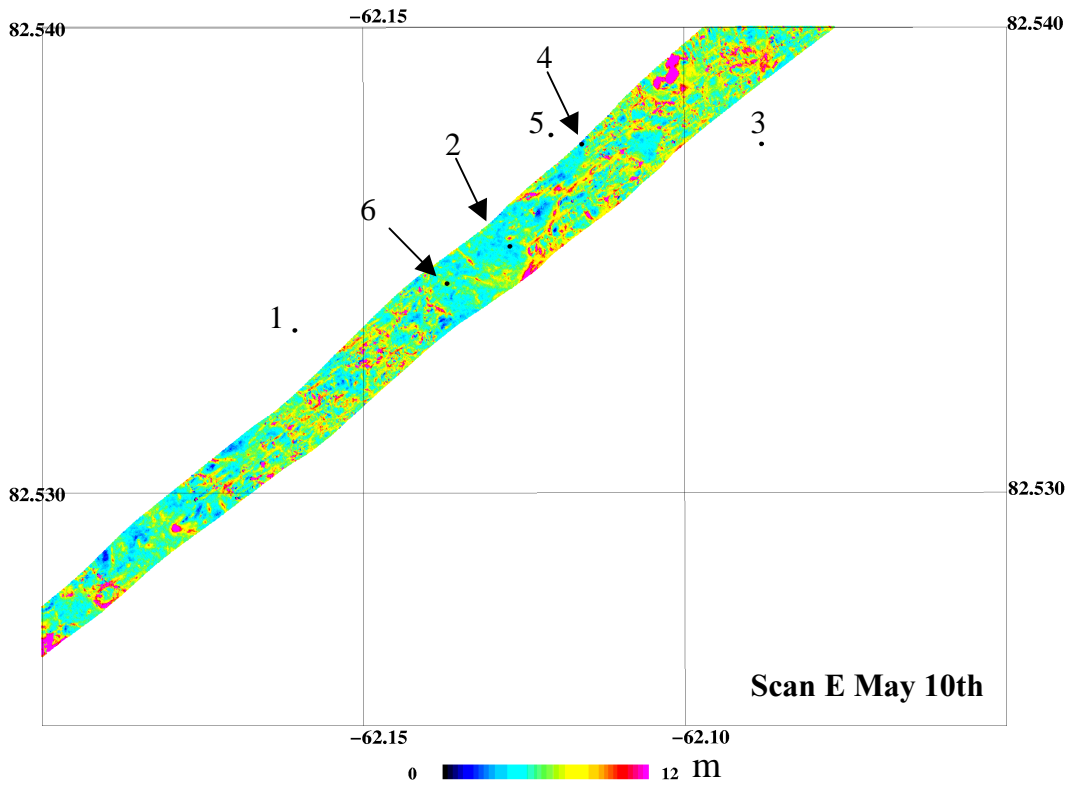
Fig 18. Comparison of laser scanner and measured thickness off Alert.

Ship-borne video – icebreaker "Oden"

ODEN carried out an oceanographic cruise in the Fram Strait and Greenland Sea in the period May 1 to June 8. With the helpful support from the crew of ODEN, an automated KMS web cam system was mounted on the bridge, taking pictures of the sea-ice at 20 sec interval, 24 hr a day, during the cruise. The images allow the occasional measurement of ice floe thickness and snow cover depth for ice floe fragments accidentally turned vertical during ice breaking. Approximately 4 GB of jpeg-imagery is available on CD-ROM archive. Fig. 20 shows the actual sailed track of Oden. Navigation data and auxiliary meteorological data have been prepared by the Oden crew, allowing geocoding of the data.

Fig. 19. Overflight of Oden ice breaker, May 6.

Figure 20. ODEN cruise tracks, May 2002. 20 sec web cam data available throughout cruise.

Fig 21. Some examples of ODEN web cam images. Scale-sitck is 2 m

The thickness of ice floes, occasionally turned vertical, can be estimated by comparing to the 'scale-stick' mounted on the side of the icebreaker, see figure 21. Each mark on the stick corresponds to 50 cm. 10 % are added to the thickness estimates to account for the distance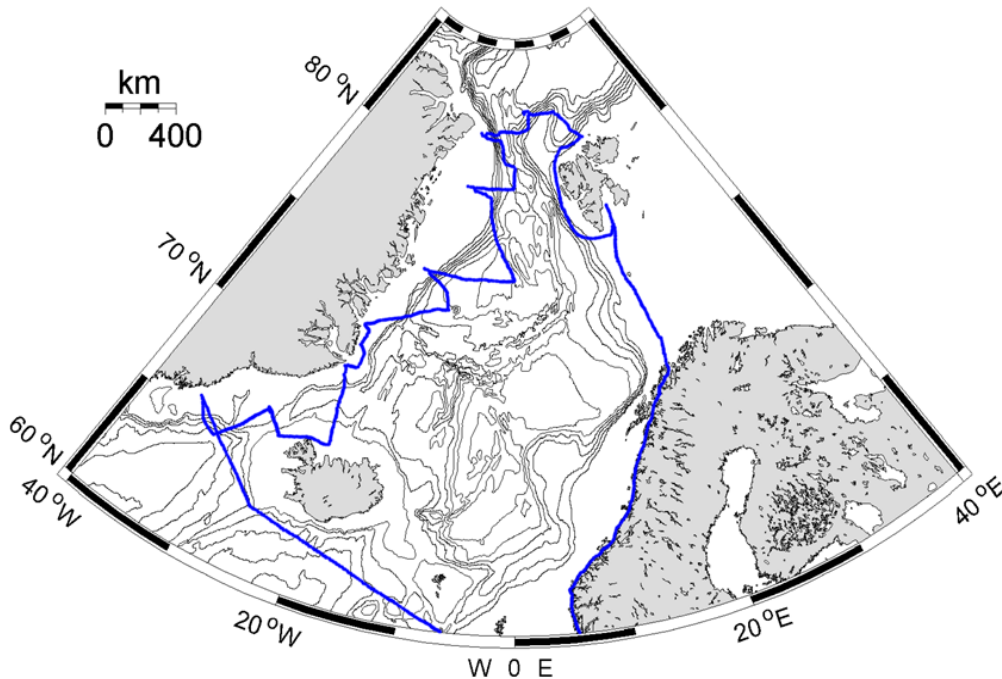 between the stick and the ice surface. Available thickness estimates from the imagery close to the aircraft tracks are shown in Fig. 22. The large differences are caused by the fact that the icebreaker only sail through the absolute thinnest parts of the ice cover, open or newly refrozen leads and thin ice. A few estimates of snow depth have also been obtained from the images giving a mean snow depth of 32 cm near the May 6th over flight of Oden.
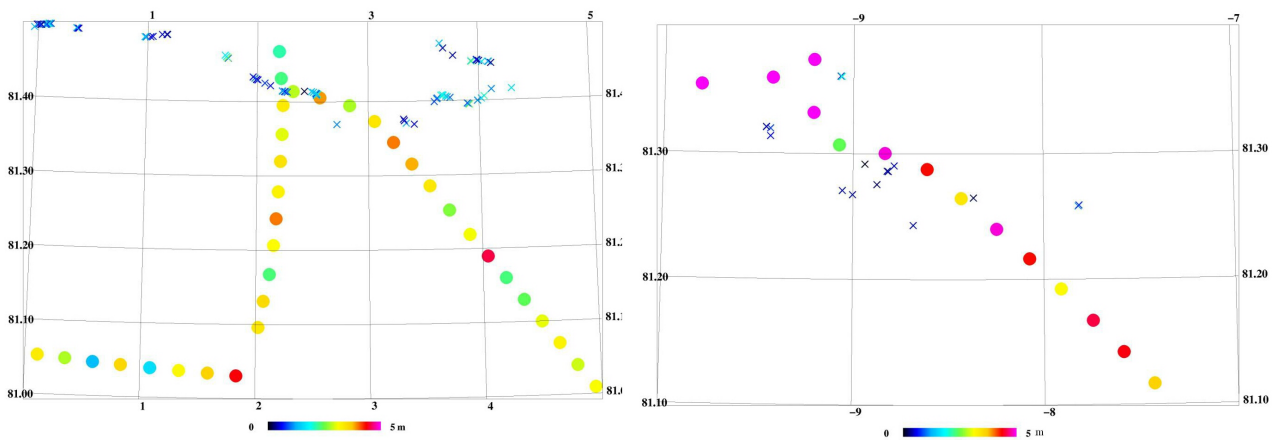
Fig. 22. Bullets: 4 km along track ice thickness estimates from laser altimetry.
X'es:Ice plus snow thickness from Oden web cam images.Left: May 6th, right: May 9th

7. CONCLUSIONS

The ESAG-2002 field campaign for airborne gravity and lidar measurements was highly successful, with nearly complete recovery of gravimetry, and a reasonable recovery of laser altimetry, given the cold weather, frequent fog and some aircraft problems.

The data material is very rich, and the final scientific processing of lidar data is far from over.

The ESAG-2002 has filled one of the last voids of the Arctic Ocean from a gravity data point of view, and the gravity data have been used in the Arctic-wide gravity compilation under the IAG "Arctic Gravity Project". The data of this project will limit the "polar gap" problem of the future GOCE gravity mission.

8. REFERENCES

Brozena, J.M., Peters, M.F., and Salman R., 1997: *Arctic airborne gravity measurement program.* Proc. International Symposium on Gravity, Geoid and Marine Geodesy, Tokyo, Sept. 1996, Springer Verlag IAG series 117.

Forsberg, R., K. Keller, S. M. Jacobsen: *Laser Monitoring of Ice Elevations And Sea-Ice Thickness in Greenland.* International Archives of Photogrammetry, Remote Sensing and Spatial Information Systems, vol. XXXIV no. 3/W4, pp. 163-169, 2001.

Forsberg, R., A. V. Olesen, K. Keller: *Airborne gravity survey of the North Greenland continental shelf.* In: Sideris, M. G. (ed): Gravity, Geoid and Geodynamics 2000, International Association of Geodesy Symposia, vol. 123, pp. 235-240, Springer Verlag, 2001.

Forsberg, R., A. V. Olesen, K. Keller, M. Møller, Arne Gidskehaug, D. Solheim: *Airborne Gravity And Geoid Surveys in the Arctic And Baltic Seas.* Proceedings of International Symposium on Kinematic Systems in Geodesy, Geomatics and Navigation (KIS-2001), Banff, June 2001, pp. 586-593.

Harlan, R. B.: *Eotvos corrections for airborne gravimetry.* J. Geophys. Res., 73, 4675-4679, 1968.

Hvidegaard, S. M. and R. Forsberg, *Sea-ice thickness from airborne laser altimetry over the Arctic Ocean north of Greenland.* Geophys. Res. Lett., 29(20), 2002

F.G. Lemoine, S.C. Kenyon, J. K. Factor, R. G. Trimmer, N.K. Pavlis, D.S. Chinn, C.M. Cox, S.M. Klosko, S. B. Luthcke, M.H. Torrence, Y.M. Wang, R.G. Williamson, E. C. Pavlis, R.H. Rapp, and T. R. Olson, *The Development of the Joint NASA GSFC and the National Imagery and Mapping Agency (NIMA) Geopotential Model EGM96*, NASA/TP-1998-206861, Goddard Space Flight Centre, Greenbelt, Maryland, July 1998.

Kenyon, S. and R. Forsberg: *Arctic Gravity Project – a status.* In: Sideris, M. G. (ed): Gravity, Geoid and Geodynamics 2000, International Association of Geodesy Symposia, vol. 123, pp. 391-395, Springer Verlag, 2001.

Olesen A V, R Forsberg, A Gidskehaug: *Airborne gravimetry using the LaCoste & Romberg gravimeter – an error analysis.* In: M.E. Cannon and G. Lachapelle (eds.). Proc. Int. Symp. on Kinematic Systems in Geodesy, Geomatics and Navigation, Banff, Canada, June 3-6, 1997, Publ. Univ. of Calgary, pp. 613-618, 1997.

Valliant, H: *The LaCoste & Romberg air/sea gravimeter: an overview.* In: CRC Handbook of Geophysical Exploration at Sea, Boca Raton Press, 1991.

ESAG2002 laser scanner files

JD	File name	2dd format	Start (dechr)	Stop	Comments
119 – April 29	112300.2dd	T	11.383	11.587	SFJ test
	113930.2dd	T	11.658	12.004	SFJ test
	145330.2dd	T	14.892	15.232	XY, SFJ-KUS
120 – April 30	104400.2dd	T	10.733	11.023	XY until landing
	110700.2dd	T	11.117	11.718	
121 – May 1	113000.2dd	T	11.500	11.790	Z, KUS-SFJ
	115200.2dd	T	11.867	12.850	
	125700.2dd	T	12.950	13.791	
122 – May 2	111700.2dd	T	11.283	12.253	A, SFJ-CNP
	121700x.2dd	T	12.283	12.676	scandisc
	125900.2dd	T	12.983	13.819	
	135000.2dd	T	13.833	14.808	
	144930.2dd	T	14.825	15.889	
123 – May 3	093330.2dd	T	9.558	10.623	Geikie
	1038300.2dd	T	10.633	11.207	
	145340.2dd	T	14.894	15.711	B, CNP-NRD
	154400.2dd	T	15.733	16.717	
	164400.2dd	T	16.733	17.720	
	174400.2dd	T	17.733	18.266	
124 – May 4	124530.2dd	T	12.758	12.836	D, NRD-NRD
	130100.2dd	T	13.017	14.092	
	140630.2dd	T	14.108	15.025	
	150230.2dd	T	15.042	16.047	
	160400.2dd	T	16.067	17.599	
	173800.2dd	T	17.633	18.035	
126 – May 6	031600.2dd	T	3.267	3.468	FG, NRD-NRD
	033700.2dd	T	3.617	4.848	
	045130.2dd	T	4.858	5.867	
	055530.2dd	T	5.892	6.842	
	065200.2dd	T	6.867	7.844	
	075130.2dd	T	7.858	8.781	
	084900.2dd	T	8.817	9.193	
	094930.2dd	T	9.825	11.204	C, NRD-LYR
	111300.2dd	T	11.217	11.911	
	115520.2dd	T	11.922	13.471	
	133000.2dd	T	13.500	13.946	
128	141740.2dd	F	14.294		syncseq not ok!
	143900.2dd	T	14.650	14.918	Kongsvegen/ Sveabreen
129 – May 9	143830.2dd	F	14.633	15.037	LYR-Nord, 1000 ft
	161030.2dd	F	16.167	17.865	
	175900.2dd	T	17.983	18.351	
130 – May 10	145210	Text – cd1	14.868	15.322	Nord-Alert

	152800	Text – cd3	15.467	15.774	
	155230	Text – cd2	15.875	16.277	
	162600	Text – cd4	16.433	16.738	
	165130	Text – cd3	16.858	17.191	
	171830.2dd	T – cd4	17.308	18.133	
	180930.2dd	T – cd1	18.150	18.917	
	185700.2dd	T – cd2	18.950	19.279	
131 – May 11	145830.2dd	T	14.975	15.337	Alert H-route
	153530.2dd	F	15.592	16.768	
	164700.2dd	T	16.783	17.759	
	174630.2dd	T	17.775	18.756	
	184630.2dd	T	18.775	19.761	
	194630.2dd	T	19.775	20.447	
132 – May 12	153900.zip	Text	15.650	16.368	Alert I-route
	163630.2dd	T	16.608	17.502	
	173100.2dd	T	17.517	18.539	
135 – May 15 first flight	124530.2dd	T - cd1	12.758	12.965	Alert G-route
	133700.2dd	T - cd2	13.616	13.480	
	143000.2dd	T - cd2	14.500	15.341	
	152130.2dd	T - cd2	15.358	16.018	
	160200.2dd	T - cd1	16.033	17.008	
	170130.2dd	T - cd1	17.025	17.997	
	181500.2dd	T - cd1	18.250	18.442	
135 – May 15 second flight	193900.2dd	T	19.650	20.040	Alert K-route
	201530.2dd	T	20.258	21.314	
	212000.2dd	T	21.333	22.361	
	222300.2dd	T	22.383	23.419	
	232600.2dd	T	23.433	24.355	
136 – May 16	122600.2dd	T – cd2	12.433	13.425	Alert J-flight
	132630.2dd	T – cd1	13.441	14.439	
	142730.2dd	T – cd1	14.458	15.369	
	152300.2dd	T – cd2	15.383	16.603	
	163700.2dd	T – cd4	16.616	17.361	
	172300.2dd	T – cd3	17.383	17.957	
137 – May 17	124500.2dd	T	12.753	12.987	Alert-Thule

APPENDIX III

Contents of "final results" CD:

SOFTWARE: readscan, fitlin, pse, pse.inp, geoid models

GRAVITY: File with final gravity anomalies

LASERALT: 2002 files + grids

LIDAR: Examples of swath freeboards
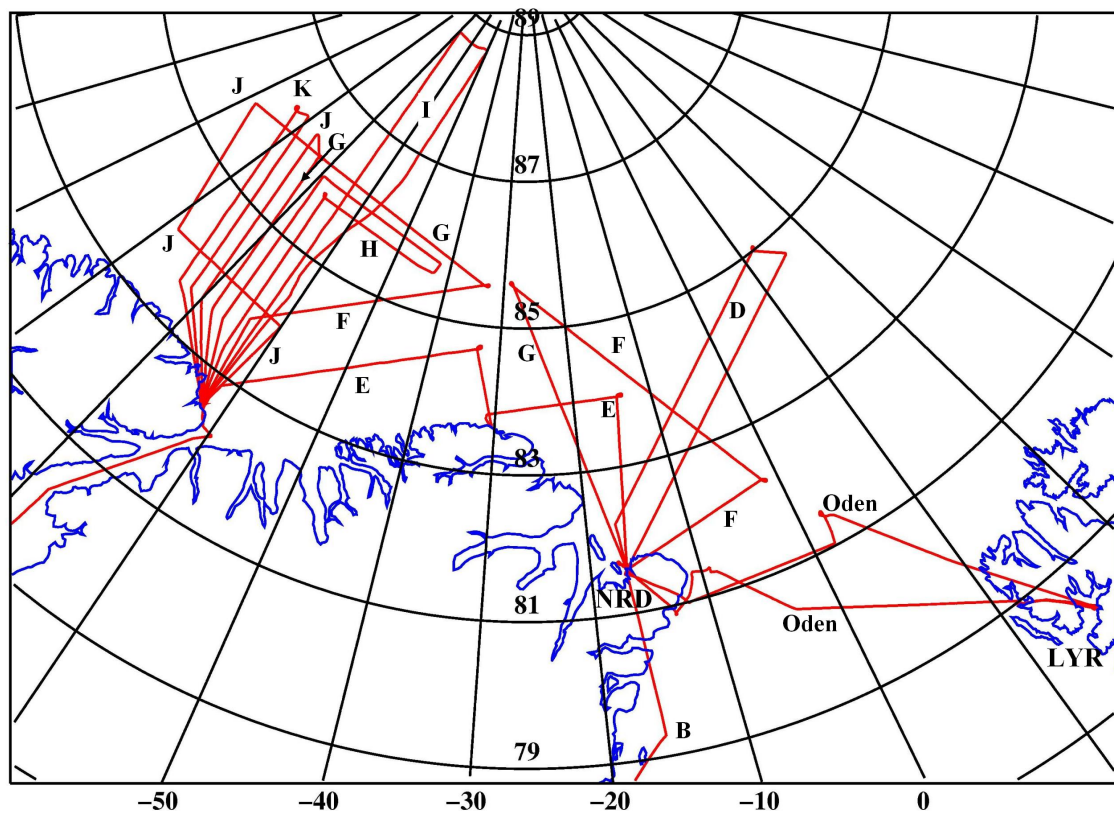
VIDEO: 5 mpegs

APPENDIX II

Fig.A3. All flights tracks of the ESAG2002 campaign.

Table A3. Flights of ESAG-2002 by Julian day and date

Date/JD	From/to	Track	Take off UTC	Landing UTC	Airborne	Operator
April 29 / 119	SFJ-SFJ	test	1131	1200	0 h 29 min	KRK
April 29 / 119	SFJ-KUS	X	1426	1818	3 h 52	KRK
April 30 / 120	KUS-KUS	X+landing, Y1 X4 X5 KUS	1041 1514 1830 2058	1149 1532 1846 2122	1 h 08 0 h 18 0 h 16 0 h 24 =2 h 06	KRK
May 01 / 121	KUS-SFJ	Z	1108	1347	2 h 39	KRK
May 02 / 122	SFJ-CNP	A	1052	1550	4 h 58	KRK
May 03 / 123	CNP-CNP	Geikie	0859	1143	2 h 44	KRK
May 03 / 123	CNP-NRD	B	1256	1850	5 h 54	KRK/SMJ
May 04 / 124	NRD-NRD	D	1248	1801	5 h 13	KRK
May 05 / 125	No flight					
May 06 / 126	NRD-NRD	F-G	0324	0917	5 h 53	KRK/SMJ
May 06 / 126	NRD-LYR	ODEN	0947	1351	4 h 04	KRK
May 07 / 127	No flight					
May 08 / 128	Test flight		1354	1502	1 h 08	AVO
May 09 / 129	LYR-NRD	ODEN	1431	1822	3 h 51	AVO
May 10 / 130	NRD-ALT	E	1411	1917	5 h 06	RF
May 11 / 131	ALT-ALT	H	1459	2025	5 h 26	AVO/SMJ
May 12 / 132	ALT-ALT	I	1420	2043	6 h 23	RF
May 13 / 133	POF to Thule for generator repair					
May 14 / 134	POF back from Thule					
May 15 / 135	ALT-ALT	F-G	1242	1827	5 h 45	AVO/SMJ
May 15 / 135	ALT-ALT	K	1943	0021	4 h 38	RF
May 16 / 136	ALT-ALT	J	1219	1756	5 h 15	AVO/SMJ
May 17 / 137	ALT-THU	L(Nares Str.)	1248	1639	3 h 51	RF/SMJ
Total					79 h 15	